ES Food and Agroforestry
DOI: https://dx.doi.org/10.30919/faf2272

Functional Characterization of Transcription Factors *PtWRKY40* and *PtWRKY69* in Jasmonic Acid-Mediated Root Rot Resistance in *Psammosilene tunicoides*

Shuyun Qi,[#] Lijuan Wang,[#] Qiaofeng Li, Fei Ji, Zhizhong Yang,[*] Guanghui Ni[*] and Aili Zhang[*]

Abstract

Root rot caused by *Fusarium oxysporum* (*F. oxysporum*) severely impacts the yield of the rare medicinal plant *Psammosilene tunicoides* (*P. tunicoides*). Previously, we identified two pathogen-responsive transcription factors, *PtWRKY40* and *PtWRKY69*, and analyzed their resistance mechanisms. LC-MS analysis revealed that *F. oxysporum* infection significantly increased jasmonic acid (JA) and methyl jasmonate (MeJA) levels in *P. tunicoides*. Concurrently, qRT-PCR showed significant upregulation of *PtWRKY40*, *PtWRKY69*, and key JA biosynthesis (*AOC1*, *AOC2*, *AOC3*) and signaling (*PtCOI1*, *PtMYC2*) genes. Subcellular localization demonstrated both *PtWRKY40* and *PtWRKY69* target the nucleus, and Y2H, BiFC, and LCI assays confirmed their physical interactions with PtMYC2. Heterologous overexpression of *PtWRKY40* and *PtWRKY69* in *Arabidopsis thaliana* significantly enhanced plant resistance to *F. oxysporum*. Furthermore, transcriptome analysis indicated that differentially expressed genes in transgenic lines were mainly enriched in defense-related pathways, including flavonoid biosynthesis and plant hormone signal transduction. This study first elucidates that *PtWRKY40* and *PtWRKY69* in *P. tunicoides* may regulate plant immunity via the JA signaling pathway to defend against *F. oxysporum* infection. These findings provide vital theoretical bases and candidate gene resources for unraveling disease resistance mechanisms and molecular breeding in *P. tunicoides*.

Keywords: *Psammosilene tunicoides*; WRKY transcription factors; Jasmonic acid; *Fusarium oxysporum*; Root rot resistance.
Received: 19 March 2026; Revised: 05 May 2026; Accepted: 13 May 2026
Article type: Research article.

1. Introduction

The traditional Chinese medicine Jintiesuo is derived from the dried roots of *Psammosilene tunicoides W.C.Wu et C.Y.Wu*, an endemic monotypic species of the Caryophyllaceae family distributed in southwestern China.[1] Pharmacological studies have demonstrated that *P. tunicoides* exhibits significant analgesic and anti-inflammatory properties. It serves as a crucial botanical ingredient in several renowned traditional Chinese patent medicines, such as Yunnan Baiyao, Baibaodan, Jingulian capsules, and Tongxuekang capsules, offering therapeutic efficacies that include dispelling wind and dampness, resolving blood stasis to relieve pain, and detoxifying to reduce swelling.[2-4] However, due to its narrow geographical distribution, slow natural growth rate, and long-term overexploitation, wild populations of *P. tunicoides* have declined drastically, pushing the species to the brink of depletion.[5] Consequently, artificial cultivation has become an essential strategy to conserve wild resources and fulfill the demands of the pharmaceutical market.

Nevertheless, during large-scale cultivation, root rot—primarily caused by soil-borne pathogenic fungi such as *Fusarium oxysporum*—has emerged as a major bottleneck restricting the development of the *P. tunicoides* industry. This disease is highly prone to outbreaks under conditions of high temperature, high humidity, and poor soil drainage. Upon infection, it causes root decay and systemic wilting, ultimately leading to plant death, which inflicts a devastating impact on both the yield and the geo-authentic quality of the medicinal materials.[6]

When coping with pathogen stress, plants activate a complex immune defense system, in which phytohormone signaling pathways play a central role in regulating disease resistance responses.[7] The jasmonic acid (JA) signaling

Yunnan Key Laboratory of Chinese Medicine Processing, Yunnan University of Chinese Medicine, Kunming, 650500, China
[#]*These authors contributed equally to this work.*
[*]*Email:* yangzhizhong@ynucm.edu.cn (Z. Yang), niguanghui@ynucm.edu.cn (G. Ni), zhangailibb@126.com (A. Zhang)

pathway primarily targets hemibiotrophic and necrotrophic fungal pathogens, conferring induced systemic resistance (ISR) to plants. In contrast, the salicylic acid (SA) signaling pathway mainly regulates systemic acquired resistance (SAR) against biotrophic pathogens.[8,9] Given that *F.oxysporum*, which causes root rot in *P. tunicoides*, is a typical hemibiotrophic fungus,[25] we hypothesize, based on empirical evidence, that the JA pathway may play a more crucial role in the resistance response of *P. tunicoides* against root rot. The JA-mediated defense response is a sequential process ranging from hormone biosynthesis to signal transduction. During the biosynthesis phase, allene oxide cyclase (*AOC*) catalyzes the conversion of unstable allene oxide into 12-oxophytodienoic acid (OPDA), representing a key step in JA biosynthesis.[10] In the signal transduction phase, the *COI1* receptor facilitates the degradation of *JAZ* repressor proteins, thereby releasing transcription factors such as *MYC2* to activate the expression of defense genes.[11] In summary, *AOC* is responsible for JA biosynthesis, while *MYC2* mediates the downstream transduction of JA signals; both play pivotal roles in the biosynthesis and signal transduction stages of the JA pathway, respectively.

WRKY transcription factors (TFs) constitute one of the largest transcription factor families.[23] Characterized by a highly conserved DNA-binding heptapeptide (WRKYGQK) and a zinc-finger motif,[12,13] they play a pivotal role in perceiving pathogen infection and remodeling the plant immune defense network.[14] Within the jasmonic acid (JA) signaling pathway, WRKY TFs can not only affect hormone accumulation levels by regulating JA biosynthesis, but also act downstream in signal transduction to modulate the expression of defense genes, serving as crucial nodes that connect pathogen recognition with immune responses.[15] Previous studies have demonstrated that in tobacco, *NaWRKY3* and *NaWRKY6* directly regulate the expression of JA biosynthesis genes (*LOX*, *AOS, AOC*, and *OPR*), thereby elevating JA levels to mediate anti-herbivore defenses;[16,17] they also function as key regulators in JA signal transduction. In *Arabidopsis thaliana*, *AtWRKY33* acts as a positive regulator of JA signaling, participating in the defense response against the necrotrophic fungus *Botrytis cinerea* by modulating the expression levels of JAZ repressor proteins.[18] Furthermore, in *Paeonia lactiflora*, *PlWRKY65* has been confirmed to participate in the defense response against *Alternaria tenuissima* by regulating the JA signaling pathway; the silencing of the *PlWRKY65* gene resulted in a significant decrease in endogenous JA levels, an increase in SA levels, and attenuated plant resistance.[19] Historically, the expression patterns of WRKY genes in response to pathogen infection have often exhibited a synergistic trend with the activation of JA pathway genes, suggesting an interaction between the two during the disease resistance process. In our preliminary research, we conducted transcriptome sequencing on field-cultivated diseased and healthy *P.tunicoides*. The results revealed that WRKY transcription factor genes were significantly differentially expressed in the diseased group. However, the molecular mechanisms underlying how WRKY transcription factors in *P. tunicoides* respond to root rot infection remain largely unclear.

In light of this, the present study was conducted with the following objectives. First, following inoculation with *F.oxysporum*, the primary pathogen of *P.tunicoides*, we determined the dynamic changes in the contents of endogenous phytohormones, jasmonic acid (JA) and salicylic acid (SA). Concurrently, the expression patterns of *PtWRKY69*, *PtWRKY40*, and key genes in the JA pathway (*AOC* and *MYC2*) were analyzed to elucidate the response relationship between *PtWRKY69/40* and the JA hormone pathway. Second, overexpression vectors for *PtWRKY69* and *PtWRKY40* were constructed and transformed into *Arabidopsis*. By inoculating the transgenic plants with necrotrophic pathogens and observing their disease resistance phenotypes, we heterologously verified the functions of these two WRKY genes in the plant disease resistance process. Finally, transcriptome sequencing technology was utilized to analyze the changes in the gene expression profiles of the WRKY-overexpressing *Arabidopsis*, thereby screening for their potential target genes. This allowed us to decipher the molecular mechanisms by which WRKY transcription factors respond to the JA signaling regulatory network to defend against root rot in *P. tunicoides*. The implementation of this project will provide a solid theoretical foundation for researching the defense mechanisms against underground diseases in medicinal plants, and offer candidate genetic resources for the molecular disease resistance breeding of *P. tunicoides*.

2. Materials and methods

2.1 Plant material cultivation

Seeds of *P.tunicoides* were collected from a cultivation base in Yuhua Village, Diannan Town, Jianchuan County, Dali, Yunnan Province, China (26.24 °N, 99.00 °E). An appropriate amount of seeds were placed into 1.5mL centrifuge tubes and surface-sterilized with a 20% seed disinfectant solution for 10 min. Subsequently, the seeds were rinsed two to four times with sterile water under a laminar flow hood and sown on Murashige and Skoog (MS) medium. The seeds were cultured under a 12-h light/12-h dark photoperiod at 23±1 ℃ with 80% relative humidity.The MS culture medium was prepared with 4.43g/L Murashige & Skoog Basal Medium with Vitamins (M519, PhytoTech Labs), supplemented with 30 g/L sucrose, 1mg/L 6-BA, 0.1 mg/L 2,4-D, and 9 g/L Agar A. The medium was sterilized by autoclaving prior to use.

An appropriate amount of *Arabidopsis* seeds was soaked in 1 mL of 20% (v/v) commercial bleach for 8 min, and then washed three times with autoclaved double-distilled water in a laminar flow hood. The seeds were sown on 1/2 Murashige and Skoog (MS) medium, stratified at 4 ℃ for 1 day, and subsequently transferred to a greenhouse for cultivation. The greenhouse conditions were maintained at a constant 22 ℃,

with a light intensity of 100μmol·m^{-2}·s^{-1} and a relative humidity of 80% under a long-day photoperiod (16 h light/8 h dark). After 7 days, the seedlings were transplanted into soil and covered with transparent plastic wrap. The wrap was removed after 2 days, and cultivation was continued. Preparation of 1/2 MS plant culture medium: The medium was prepared by dissolving 10 g/L sucrose and 2.22 g/L Murashige and Skoog Basal Medium with Vitamins (M519, PhytoTech Labs). After adjusting to the final volume, the pH was adjusted to 5.80. Subsequently, 8 g/L Agar A was added, and the medium was sterilized by autoclaving.

Nicotiana benthamiana was used as the experimental plant material. A growth substrate consisting of potting soil and vermiculite in a 5:1 ratio was thoroughly moistened with an aqueous solution containing Murashige and Skoog (MS) basal salts and then filled into seedling trays. The seeds were evenly sown on the surface of the substrate and covered with transparent domes to retain moisture. The plants were cultivated under a 16-h light/8-h dark photoperiod at 22–25 ℃ with a relative humidity of 75%–85%.

When the seedlings developed two to three true leaves, they were transplanted into individual pots. During the initial stage of transplantation, the seedlings were kept covered to maintain high humidity. Subsequently, the humidity was gradually reduced to acclimate the plants to standard growth conditions. After an additional 20 to 30 days of growth, the plants were used for subsequent transient expression assays.

2.2 Pathogen source and inoculation treatments

The pathogenic strain *F.oxysporum* PSD-3 used in this study was previously isolated and purified by our research group from the junction of diseased and healthy root tissues of *P.tunicoides* plants exhibiting root rot symptoms in Yunnan Province. Its pathogenicity had been verified according to Koch's postulates, and the strain was identified based on colony morphology, conidial characteristics, and sequence analysis of the internal transcribed spacer (ITS) and translation elongation factor 1-alpha (TEF-1α) genes.[20] This strain was maintained in our laboratory for subsequent inoculation assays.

Three-week-old tissue-cultured seedlings of *P. tunicoides* were used as plant materials. The seedlings were inoculated using the root-dipping method with 1 mL of an *F. oxysporum* conidial suspension at a concentration of 5* 10^⁶ conidia/mL. Uninoculated seedlings were used as the mock control.

2.3 Quantification of endogenous phytohormones

Whole *P.tunicoides* seedlings were harvested at 24 h post-inoculation with *F. oxysporum*, and mock-inoculated seedlings were used as the control. Endogenous phytohormones were extracted from the samples using acetonitrile and subsequently purified via the QuEChERS method. The simultaneous quantification of multiple phytohormones was conducted using an ultra-performance liquid chromatography (UPLC; Qsight LX 50, PerkinElmer, USA) system coupled with a triple quadrupole mass spectrometer (QQQ-MS; Qsight 420, PerkinElmer, USA). To ensure accurate quantification, internal standards were added to the extraction solvent for correction, and the final concentrations were determined based on the internal standard method. All analyses included control groups and were performed with three independent biological replicates. Statistical differences between groups were evaluated using Student's t-test ($p < 0.05$; $p < 0.01$).

2.4 qRT-pcr analysis

Total RNA was extracted from wild-type *P.tunicoides* plants treated with *F.oxysporum* for 3, 6, 12 h, and reverse-transcribed into cDNA. The qRT-PCR method was applied to analyze the effect of *F. oxysporum* inoculation treatment on gene expression changes. The qRT-PCR was performed by Beijing Tsingke Biotechnology Co., Ltd.[21] The primers used in this study were designed using Primer 5.0 software, and the primer sequences are listed in Table S1. All detections included a control group and utilized three independent biological replicates.

2.5 Gene cloning

Total RNA was extracted from the leaves of three-week-old tissue-cultured *P. tunicoides* seedlings using a Plant Total RNA Extraction Kit (Tiangen, Beijing, China), and subsequently reverse-transcribed into cDNA using a reverse transcription kit. Gene-specific primers for *PtWRKY40*, *PtWRKY69*, and *PtMYC2* were designed based on their target sequences. The target fragments were amplified from the genomic cDNA using the primers. The PCR amplification program was as follows: initial denaturation at 95 °C for 5 min, followed by 34–36 cycles of 95 °C for 30 s, 60 °C for 30 s, and 72 °C for 5 min. The PCR products were cloned into the 101 vector driven by the strong CaMV 35S promoter, and confirmed by sequencing. Simultaneously, the respective target genes were also inserted into corresponding vectors for subcellular localization, yeast two-hybrid (Y2H), bimolecular fluorescence complementation (BiFC), and luciferase complementation imaging (LCI) assays to evaluate protein localizations and physical interactions.

2.6 Subcellular localization analysis

The successfully constructed subcellular localization vectors, *35S::PtWRKY40-GFP* and *35S::PtWRKY69-GFP*, were transformed into *Agrobacterium tumefaciens* strain GV3101 competent cells. Positive single clones were selected and inoculated into Luria-Bertani (LB) liquid medium containing appropriate antibiotics, followed by shaking culture at 200 rpm and 28 °C for 16 h. The optical density at 600 nm (OD_{600}) of the bacterial culture was measured. A 1-mL aliquot of the culture was centrifuged at 10,000 × g for 1 min. After discarding the supernatant, the pellet was resuspended in MMA buffer, and the OD_{600} of the bacterial suspension was adjusted to 0.5. The resuspended cells were incubated in the dark at 28 °C for 2 h and subsequently infiltrated into the abaxial surface of *N.benthamiana* leaves using a 1-mL

needleless syringe. At 48 h post-infiltration, the leaves were infiltrated with DAPI solution and incubated in the dark for 30 min. The GFP and DAPI fluorescence signals were observed and photographed using a confocal laser scanning microscope (CLSM).

2.7 Yeast two-hybrid assay

To verify the protein-protein interactions between PtMYC2 and *PtWRKY40*/*PtWRKY69*, the open reading frames (ORFs) of *PtWRKY40* and *PtWRKY69* were cloned into the pGADT7 (AD) prey vector, respectively, while the ORF of *PtMYC2* was cloned into the pGBKT7 (BD) bait vector. Different combinations of recombinant plasmids were co-transformed into the yeast competent cell strain Y2HGold using the PEG/LiAc method. The transformants were initially plated on double dropout medium (SD/–Leu/–Trp) and incubated at 28 °C for 2–3 days to screen for positive yeast transformants. Subsequently, single colonies with consistent growth were selected and plated onto quadruple dropout medium (SD/–Leu/–Trp/–His/–Ade). Due to a certain degree of transcriptional autoactivation of the bait vector, 30 mM 3-amino-1,2,4-triazole (3-AT) was supplemented into the quadruple dropout medium to suppress background growth. Yeast growth was observed and recorded after 3–5 days of incubation at 28 °C. Co-transformations with corresponding empty vectors were included as negative controls. The normal growth of the tested transformants on the quadruple dropout medium supplemented with 3-AT was considered indicative of a positive protein-protein interaction.

2.8 Bimolecular fluorescence complementation assay (BiFC)

To verify the in planta protein-protein interactions between PtMYC2 and *PtWRKY40*/*PtWRKY69*, the target genes were individually cloned into the BiFC vectors pAB862-NYFP and pAB855-CYFP to generate corresponding recombinant plasmids. The sequence-verified recombinant vectors were transformed into *Agrobacterium tumefaciens* strain GV3101 competent cells.The procedures for Agrobacterium cultivation, cell harvesting, resuspension in MMA buffer, and infiltration into *N.benthamiana* leaves were identical to those described for the subcellular localization assays. For co-infiltration, the appropriate pairs of bacterial suspensions were mixed in equal volumes (1:1, v/v), and the final OD_{600} of the mixture was adjusted to 0.8. After a 2-h dark incubation at 28 °C, the mixtures were co-infiltrated into the leaves. At 48 h post-infiltration , the leaves were stained with DAPI solution and incubated in the dark for 30 min. The reconstituted fluorescence signals were observed and photographed using a confocal laser scanning microscope (CLSM). Co-infiltrations with corresponding empty vectors were included as negative controls.

2.9 Dual-luciferase complementation imaging assay (LCI)

To further verify the in planta protein-protein interactions between PtMYC2 and *PtWRKY40*/*PtWRKY69*, the open reading frames (ORFs) of *PtWRKY40* and *PtWRKY69* were cloned into the pCAMBIA-cLUC vector, respectively, while the ORF of PtMYC2 was cloned into the pCAMBIA1300-nLUC vector to generate the corresponding recombinant plasmids. The sequence-verified recombinant vectors were transformed into *Agrobacterium tumefaciens* strain GV3101 competent cells.The procedures for Agrobacterium cultivation, cell harvesting, resuspension in MMA buffer, and leaf infiltration were identical to those described for the subcellular localization assays. For co-infiltration, the appropriate pairs of bacterial suspensions were mixed in equal volumes (1:1, v/v), and the final OD_{600} of the mixture was adjusted to 1.0. After a 2-h dark incubation at 28 °C, the mixtures were co-infiltrated into the *N.benthamiana* leaves. At 48 h post-infiltration (hpi), the luciferase substrate D-luciferin was applied to the infiltrated areas. Following a 3–5 min incubation in the dark, luminescence signals were detected and photographed using a Tanon 5200 Multi imaging system. Co-infiltrations with corresponding empty vectors were included as negative controls.

2.10 Agrobacterium-mediated transformation of *Arabidopsis*

The recombinant plasmids *101-WRKY40/69* were transformed into Agrobacterium tumefaciens (GV3101) and introduced into 4-week-old *Arabidopsis* (wild-type) plants using the Agrobacterium-mediated floral dip method. After obtaining the T1 generation seeds, the transgenic plants were screened on MS medium containing 50 mg/L kanamycin. PCR and RT-PCR were performed using genomic DNA and cDNA samples, respectively, to verify the transgenic plants, with wild-type DNA and cDNA serving as controls. The amplification conditions were an initial 95 ℃ for 5 min, 95 ℃ for 30 s, 60 ℃ for 30 s, and 72 ℃ for 5 min.

2.11 Pathogen cultivation and *Arabidopsis* phenotypic experiment

F.oxysporum was cultured in potato dextrose broth (PDA) medium on a shaker at 28 ℃ for 4 days. Conidia were harvested by centrifugation and washed with sterile water; the final concentration was adjusted to 5*10^6conidia/mL using a hemocytometer. Leaves from 3-week-old *Arabidopsis* were excised and inoculated with *F. oxysporum*. At 5-7 days post-inoculation, the leaf lesion area was measured using image software.

2.12 Transcriptome sequencing analysis of *PtWRKY40/69* Arabidopsis

2.12.1 Total RNA extraction, purification, and quality detection

Total RNA from the leaves of nine frozen *Arabidopsis* (*W40-OE*, *W69-OE*, and WT, totaling three treatment groups with three samples per group) was extracted using the TRIzol total RNA extraction kit. The concentration and purity of RNA were

detected using a Nanodrop 2000 spectrophotometer, and RNA integrity was detected by agarose gel electrophoresis. Simultaneously, an Agilent 5300 was used to determine the RQN value for quality assessment. Samples with an OD260/280 ratio ranging from 1.8 to 2.2 and an RQN > 6.5 were used for subsequent analysis.

2.12.2 cDNA library construction and transcriptome sequencing

The construction and sequencing of the nine cDNA libraries were performed by Shanghai Majorbio Bio-pharm Technology Co., Ltd. (Shanghai, China). A total amount of 1 ug of qualified RNA per sample was used as input material for the library preparation. According to the manufacturer's protocol, sequencing libraries were generated on the illumina X-Plus sequencing platform. The main procedures were as follows: First, mRNA was separated from the total RNA using Oligo (dT) magnetic beads based on A-T base pairing with ployA. Under elevated temperature conditions, fragmentation buffer was added to randomly cleave the mRNA into short fragments of approximately 300 bp. The RNA fragments were reverse-transcribed into first-strand cDNA using reverse transcriptase, followed by second-strand cDNA synthesis. Subsequently, End Repair Mix was added to blunt the double-stranded ends, an A base was added to the 3' ends, and the fragments were size-selected and purified using magnetic beads. Finally, PCR amplification was performed to construct the sequencing library.

2.12.3 Sequencing data quality control and sequence alignment analysis

The raw sequencing data underwent quality filtering to remove sequences containing adapters, low-quality reads, and sequences with an excessively high proportion of N bases, thereby obtaining high-quality effective sequencing data (clean reads). Trinity software (https://github.com/trinityrnaseq/trinityrnaseq/wiki) was employed to perform de novo assembly on the cleandata of all samples, and the longest transcript of each gene after assembly was taken as the unigene. The BLAST tool was used to align the clean reads of each sample with the reference sequences obtained from the Trinity assembly, resulting in sequence clusters. Functional annotation and classification of the unigene sequences were performed through six major databases: NR, Swiss-Prot, Pfam, EggCOG, KECG, and GO.

Gene expression levels were quantified using RSEM software, and differential expression analysis between sample groups was performed using DESeq2 software. The screening thresholds were set at |log2(FoldChange)| > 1 and q-value< 0.05, ultimately yielding the differentially expressed gene sets between the groups.[22]

3. Results and discussion

3.1 Validation of the activation of phytohormone signaling pathways in *P.tunicoides* under pathogen stress

To verify the effectiveness of the inoculation treatment, we first observed the phenotypic changes in the roots of *P. tunicoides* at 24 h post-inoculation (hpi). As shown in Fig. 1A, compared with the uninoculated control (CK), the leaves of the plants inoculated with *F.oxysporum* exhibited obvious yellowing and wilting, whereas the leaves of the control group remained robust without visible lesions, indicating the successful infection of *P. tunicoides* by the pathogen. To elucidate the hormone regulatory network of *P.tunicoides* in

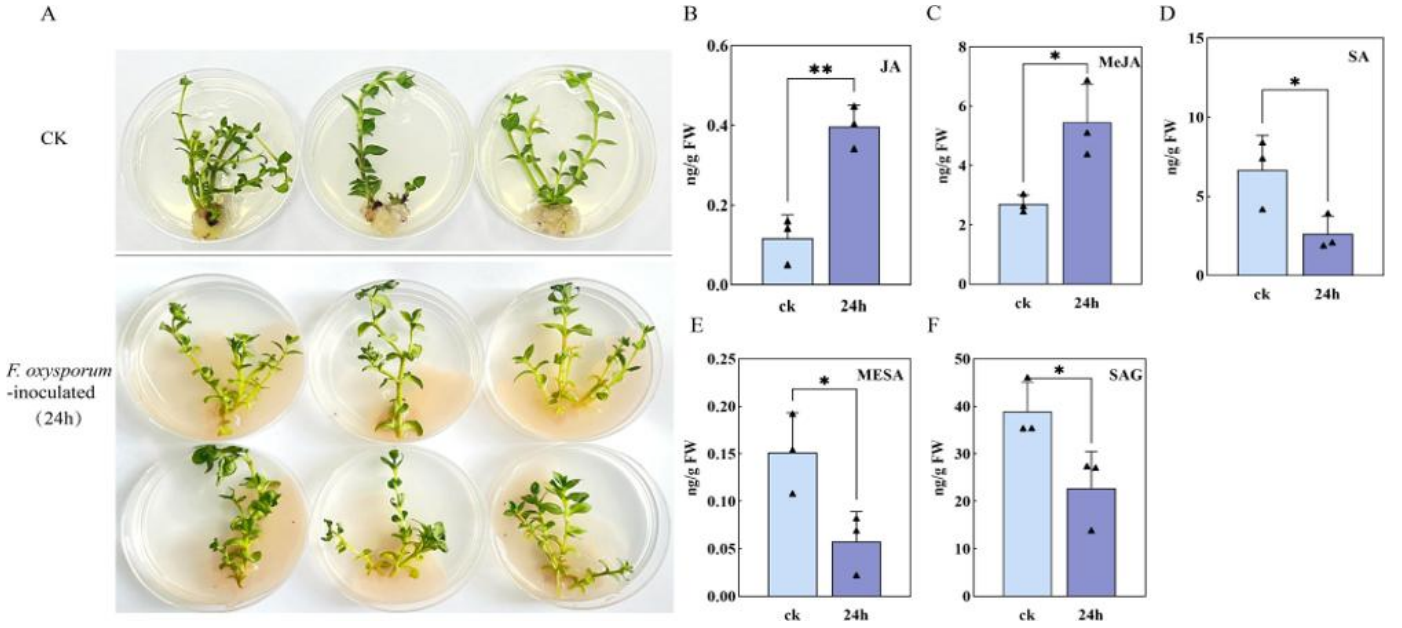


Fig. 1: Phenotypic changes and endogenous hormone contents in *P.tunicoides* at 24 h after inoculation with *F.oxysporum*.(A) Phenotypes of *P. tunicoides* after inoculation with *F. oxysporum*; (B-F) Changes in the contents of JA, MeJA, SA, MeSA, and SAG in *P. tunicoides* at 24 h after inoculation, as determined by LC-MS. Data represent the mean of three independent biological replicates. Statistical significance was analyzed using Student's t-test (P < 0.05, *P < 0.01).

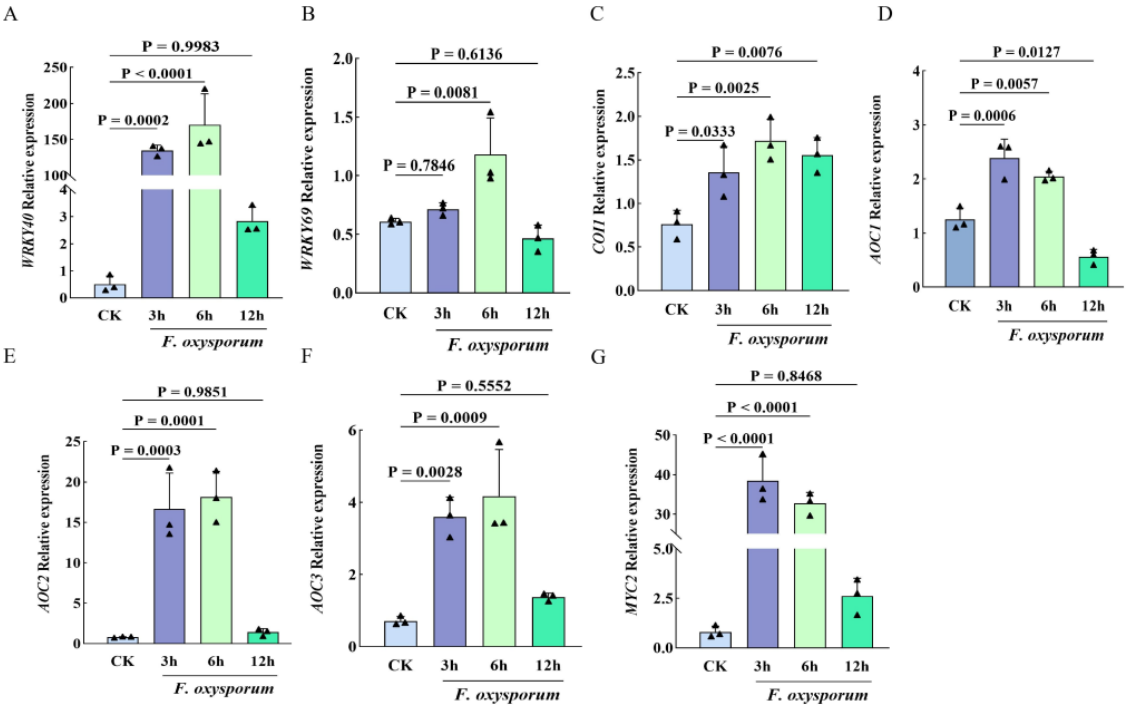


Fig. 2: Expression levels of *PtWRKY40*, *PtWRKY69*, and key genes of the JA pathway (*COI1*, *AOC1*, *AOC2*, *AOC3*, and *MYC2*) in *P.tunicoides* at 3, 6, and 12 h post-inoculation with *F.oxysporum* analyzed by qRT-PCR (A-G). Data represent three independent biological replicates. Statistical significance was analyzed using Student's t-test (*P < 0.05; **P < 0.01).

response to the root rot pathogen (*F.oxysporum*) infection, we measured the dynamic changes in the contents of jasmonic acid (JA), methyl jasmonate (MeJA), salicylic acid (SA), and its primary metabolites methyl salicylate (MeSA) and salicylic acid glucoside (SAG) in the roots at 24 hpi. As illustrated in Figure , compared with the control group (CK), pathogen infection significantly induced the accumulation of JA, with its content increasing from approximately 0.1 ng/g FW (fresh weight) in the control to approximately 0.4 ng/g FW, representing a significant difference ($p < 0.01$) (Fig. 1B). Simultaneously, the content of MeJA, the active form of JA, also showed a significant upward trend ($p < 0.05$) (Fig. 1C), demonstrating that the JA signaling pathway was rapidly activated during the early stage of infection. Conversely, the SA signaling pathway exhibited a suppressed trend. At 24 hpi, the free SA content was significantly lower than that of the control group ($p < 0.05$), and the contents of its volatile derivative MESA and bound storage form SAG also decreased significantly ($p < 0.05$) (Fig. 1D-F). The above results indicate that infection by the root rot pathogen (a necrotrophic pathogen) preferentially activated the JA signaling pathway and significantly downregulated the SA pathway in *P. tunicoides*. This is consistent with the typical hormone response pattern (JA↑/SA↓) induced by necrotrophic pathogens, suggesting that the JA-mediated defense response may play a dominant role in the resistance of *P. tunicoides* to root rot.

3.2 Expression of *PtWRKY40/69* and JA pathway-related genes induced by pathogen stress

To further investigate the regulatory relationship between the JA signaling pathway and WRKY transcription factors, we employed qRT-PCR to analyze the expression levels of *PtWRKY40*, *PtWRKY69*, and key genes of the JA pathway in *P.tunicoides* plants at different time points (3 h, 6 h, and 12 h) post-inoculation. As shown in Fig. 2A, *PtWRKY40* was strongly induced at the early stage of infection, with its expression levels upregulated by approximately 3-fold and 6-fold at 3 h and 6 h, respectively, compared to the control ($p < 0.0001$). Although its expression decreased at 12 h, it remained significantly higher than that of the control ($p < 0.0001$). *PtWRKY69* was significantly upregulated at 6 h ($p < 0.0001$) (Fig. 2B), while its expression levels at 3 h and 12 h showed no significant difference compared to the control ($p > 0.05$), exhibiting a different dynamic expression pattern from that of *PtWRKY40*. Expression analysis of genes related to the JA signaling pathway revealed (Fig. 2C-G) that the JA receptor gene *COI1* was continuously and significantly upregulated at 3 h, 6 h, and 12 h ($p < 0.01$), indicating that the JA signal perception mechanism was rapidly activated following pathogen recognition. The key JA biosynthesis gene *AOC1* was significantly upregulated at 3 h ($p < 0.01$), maintained a relatively high level at 6 h, and exhibited decreased expression at 12 h. Meanwhile, *AOC2* and *AOC3* were significantly upregulated at both 3 h and 6 h ($p < 0.001$), followed by a decrease in expression at 12 h. The core transcription factor of JA signaling, *MYC2*, was significantly elevated at 3 h ($p < 0.0001$), and gradually decreased at 6 h and 12 h, although it remained higher than the control.

The aforementioned results demonstrate that the JA

signaling pathway in *P.tunicoides* was rapidly activated following pathogen infection. The JA biosynthesis genes (*AOC1*, *AOC2*, and *AOC3*) and signal transduction components (*COI1* and *MYC2*) were significantly upregulated as early as 3 h post-inoculation. Similarly, *PtWRKY40* was significantly induced at 3 h and reached its peak expression at 6 h, while *PtWRKY69* was significantly upregulated at 6 h. Therefore, we hypothesize that *PtWRKY40* and *PtWRKY69* may participate in the defense response of *P. tunicoides* against the root rot pathogen via the JA signaling pathway in distinct temporal patterns.

3.3 Subcellular localization analysis of *PtWRKY40*/69

To determine the subcellular localization of the *PtWRKY40* and *PtWRKY69* proteins, we constructed transient expression vectors tagged with green fluorescent protein (GFP). Using homologous recombination, the coding sequences of *PtWRKY40* and *PtWRKY69* were individually cloned into the WMV047-GFP vector to generate the 35S::*PtWRKY40*-GFP and 35S::*PtWRKY69*-GFP fusion expression constructs. These constructs, along with the empty 35S::GFP vector acting as a control, were transiently expressed in *N.benthamiana* leaves, and the GFP fluorescence was observed. As shown in Fig. 3, the fluorescence signals of the empty 35S::GFP control were ubiquitously distributed throughout the cells, whereas the green fluorescence of 35S::*PtWRKY40*-GFP and 35S::*PtWRKY69*-GFP was exclusively detected in the nucleus. These results demonstrate that both *PtWRKY40* and *PtWRKY69* are nuclear-localized proteins.

3.4 Validation of the Interactions Between *PtWRKY40*/69 and PtMYC2

To verify the protein-protein interactions between PtMYC2 and *PtWRKY40*/*PtWRKY69*, yeast two-hybrid (Y2H), bimolecular fluorescence complementation (BiFC), and luciferase complementation imaging (LCI) assays were conducted. The Y2H results (Fig. 4) showed that, after supplementing the selective medium with 30 mM 3-AT to suppress the autoactivation of the bait vector, yeast cells co-expressing the *PtWRKY40*/PtMYC2 and *PtWRKY69*/PtMYC2 combinations grew normally, whereas the negative controls failed to grow. These results demonstrate that both *PtWRKY40* and *PtWRKY69* physically interact with PtMYC2.

To further validate these interactions in planta, bimolecular fluorescence complementation (BiFC) assays were performed. As shown in Fig. 5 strong reconstituted YFP fluorescence

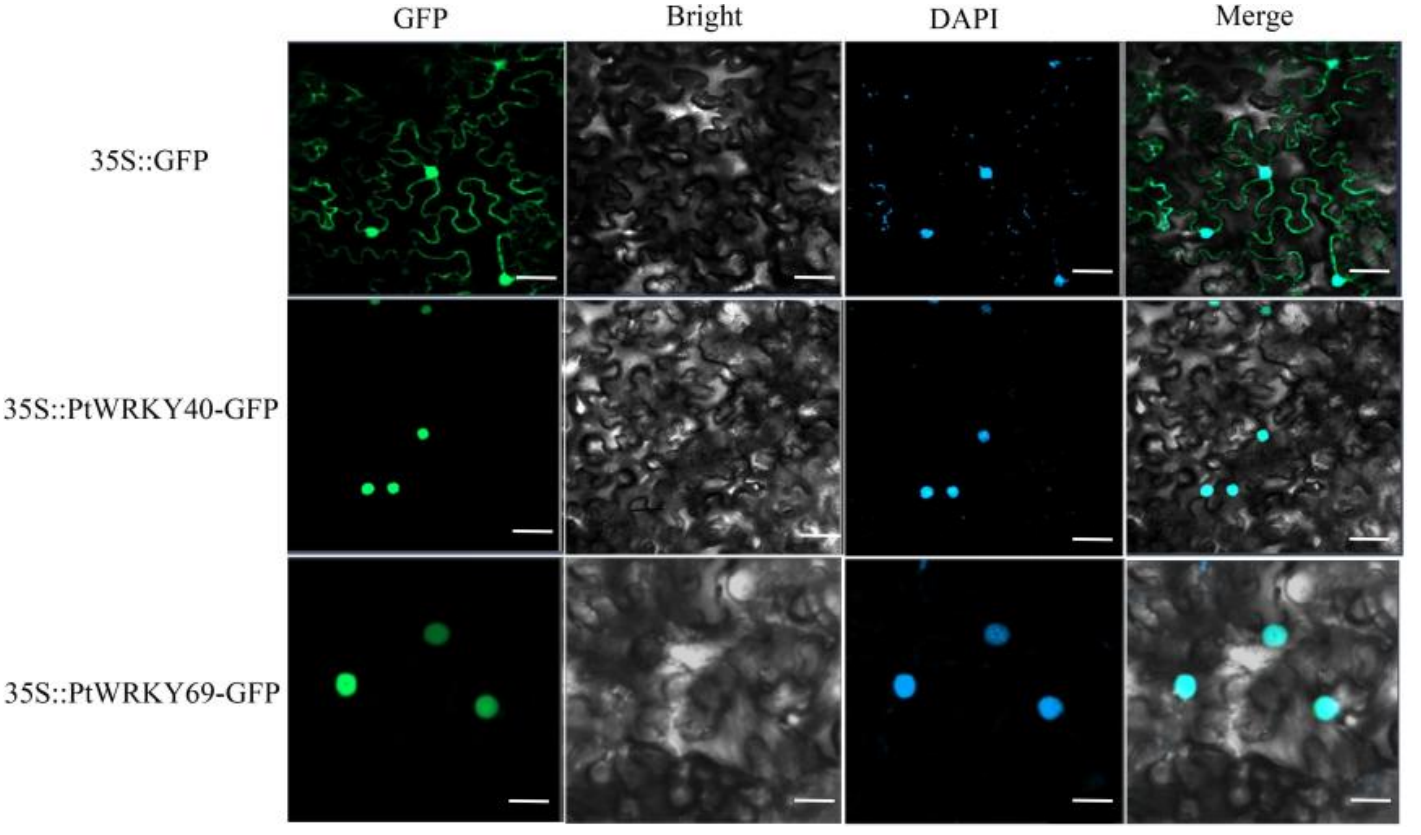


Fig. 3: Subcellular localization of PtWRKY40 and PtWRKY69 in *N.benthamiana* leaves.The recombinant constructs 35S::PtWRKY40-GFP and 35S::PtWRKY69-GFP were transiently expressed in *N.benthamiana* leaves, with the empty 35S::GFP vector acting as a control. At 48 h post-infiltration (hpi), the leaves were stained with DAPI, and GFP fluorescence signals were observed using a confocal laser scanning microscope (CLSM). Green fluorescence indicates the GFP signals, and blue fluorescence indicates the DAPI-stained nuclei. Merge represents the overlaid images of the fluorescence and bright-field channels. Scale bars = 50μm.

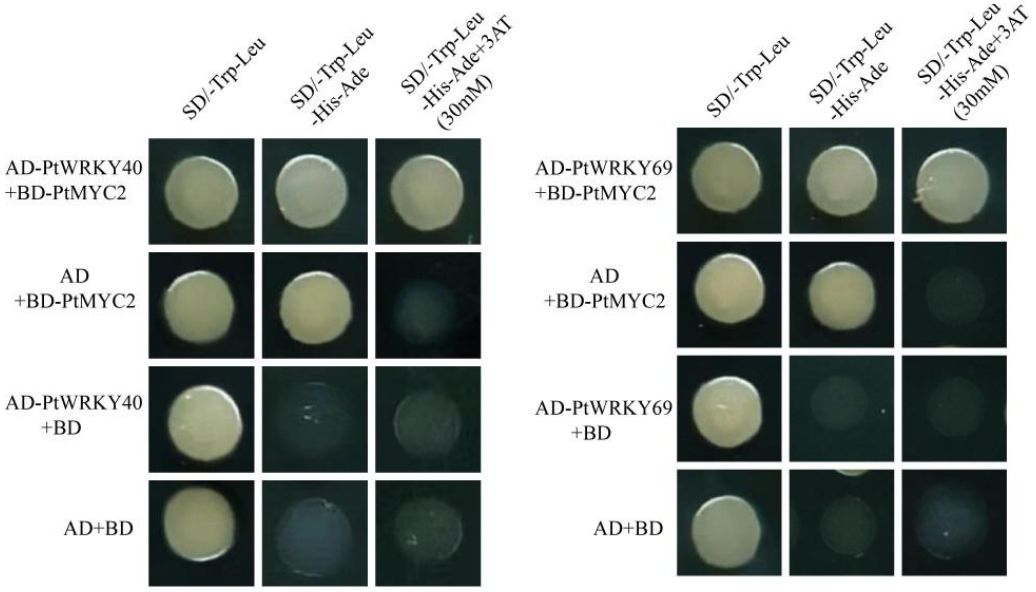


Fig. 4: Yeast two-hybrid (Y2H) assays.The left panel shows the interaction between AD-PtWRKY40 and BD-PtMYC2 alongside their negative controls, while the right panel displays the interaction between AD-PtWRKY69 and BD-PtMYC2 alongside their negative controls. Co-transformed yeast cells were spotted onto double dropout (SD/–Trp/–Leu) medium, quadruple dropout (SD/–Trp/–Leu/–His/–Ade) medium, and quadruple dropout medium supplemented with 30 mM 3-AT to evaluate the protein interactions. AD and BD indicate the empty vector controls.

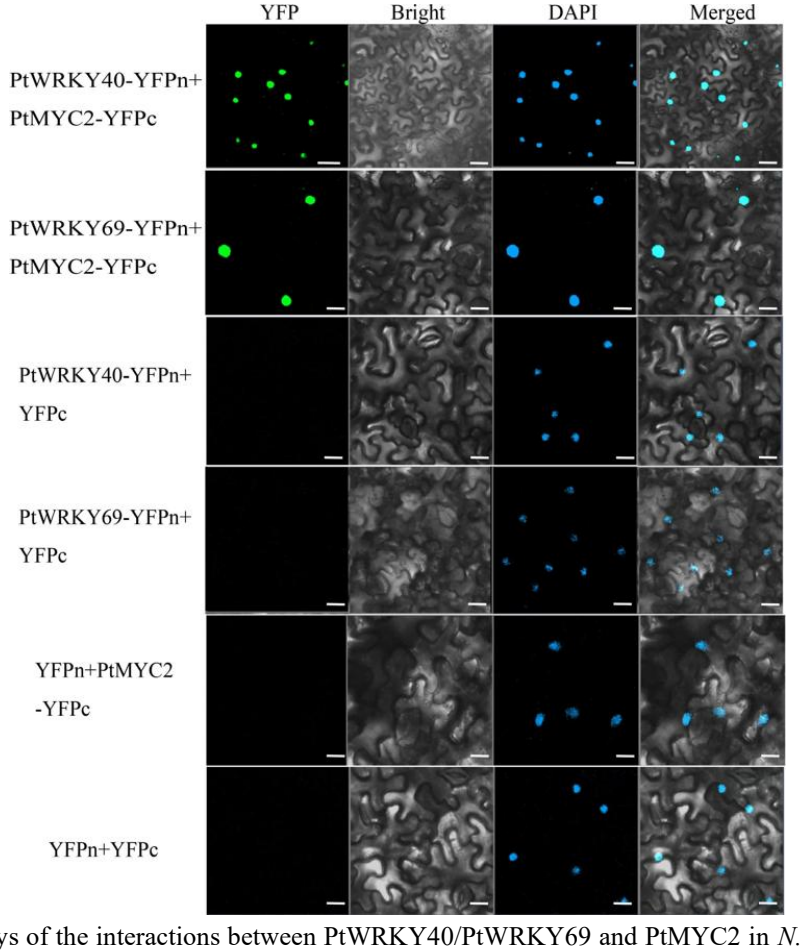


Fig. 5: BiFC assays of the interactions between PtWRKY40/PtWRKY69 and PtMYC2 in *N.benthamiana* leaves. Agrobacterium suspensions harboring the corresponding recombinant constructs were mixed in equal volumes and co-infiltrated into *N.benthamiana* leaves. At 48h post-infiltration (hpi), the leaves were stained with DAPI, and the reconstituted YFP fluorescence signals were observed using a confocal laser scanning microscope (CLSM). No obvious fluorescence signals were detected in the negative controls. Scale bars = 15 μm.

signals were observed in *N.benthamiana* leaf cells co-expressing *PtWRKY40* with PtMYC2, as well as *PtWRKY69* with PtMYC2. Conversely, no obvious fluorescence signals were detected in the negative controls. Notably, these fluorescence signals were predominantly localized to the nucleus. These findings demonstrate that both *PtWRKY40* and *PtWRKY69* physically interact with PtMYC2 within living plant cells.

To further validate these findings, luciferase complementation imaging (LCI) assays were performed to assess the interactions between PtMYC2 and *PtWRKY40*/*PtWRKY69*. As shown in Fig. 6, distinct luminescence signals were generated in *N.benthamiana* leaves co-infiltrated with *PtWRKY40* and PtMYC2, as well as with *PtWRKY69* and PtMYC2. In contrast, no obvious luminescence was detected in the negative controls. These results further confirm that both *PtWRKY40* and *PtWRKY69* physically interact with PtMYC2 in planta.

3.5 Heterologous expression of *PtWRKY40/69* enhances resistance to *F. oxysporum* in *Arabidopsis*

To verify the functions of *PtWRKY40* and *PtWRKY69* in disease resistance responses, overexpression constructs *101-wrky40* and *101-wrky69* driven by the CaMV 35S promoter were transformed into wild-type (Col-0) *Arabidopsis* using the Agrobacterium-mediated transformation method. Following resistance screening (Kanamycin), T1 generation positive plants were obtained. Genomic PCR detection confirmed that the target genes had been integrated into the *Arabidopsis* genome (Fig. 7A). Homozygous overexpression lines, *W40-OE* and *W69-OE*, with transcription levels significantly higher than those of the wild-type (WT), were further screened by qRT-PCR (Fig. 7B) for disease resistance evaluation. A leaves inoculation method was employed to analyze the resistance of T3 generation transgenic and WT plants to *F.oxysporum*. At 5-7 days post-inoculation (dpi), the leaves of WT plants exhibited obvious lesions, yellowing, and wilting, whereas the disease severity in the overexpression lines was significantly alleviated. Quantification of leaf lesion areas revealed that the overexpression lines exhibited significantly smaller lesions compared to the wild type. (Fig. 7C). These results demonstrate that the overexpression of *PtWRKY40* and *PtWRKY69* significantly enhanced the resistance of *Arabidopsis* to *F.oxysporum*.

3.6 Transcriptome analysis of *PtWRKY40/69* overexpression lines

3.6.1 Transcriptome sequencing results and quality assessment

WRKY transcription factors play crucial roles in plant disease resistance. In the model plant *Arabidopsis*, several WRKY transcription factors have been cloned and functionally characterized; however, WRKY transcription factors in *P.tunicoides* have not yet been reported. To explore the disease resistance functions of *PtWRKY40* and *PtWRKY69* from *P.tunicoides*, we constructed transgenic *Arabidopsis* lines overexpressing *PtWRKY40* (*W40-OE*) and *PtWRKY69* *(W69-OE)* and performed whole-transcriptome analysis on their leaf tissues, aiming to further elucidate the regulatory mechanisms underlying the disease resistance mediated by *PtWRKY40* and *PtWRKY69*.

RNA-Seq analysis was performed on the leaves of *W40-OE* and *W69-OE* transgenic *Arabidopsis* to reveal the potential disease resistance mechanisms underlying the overexpression of WRKY transcription factors in the plants.

Three biological replicates were included for both the

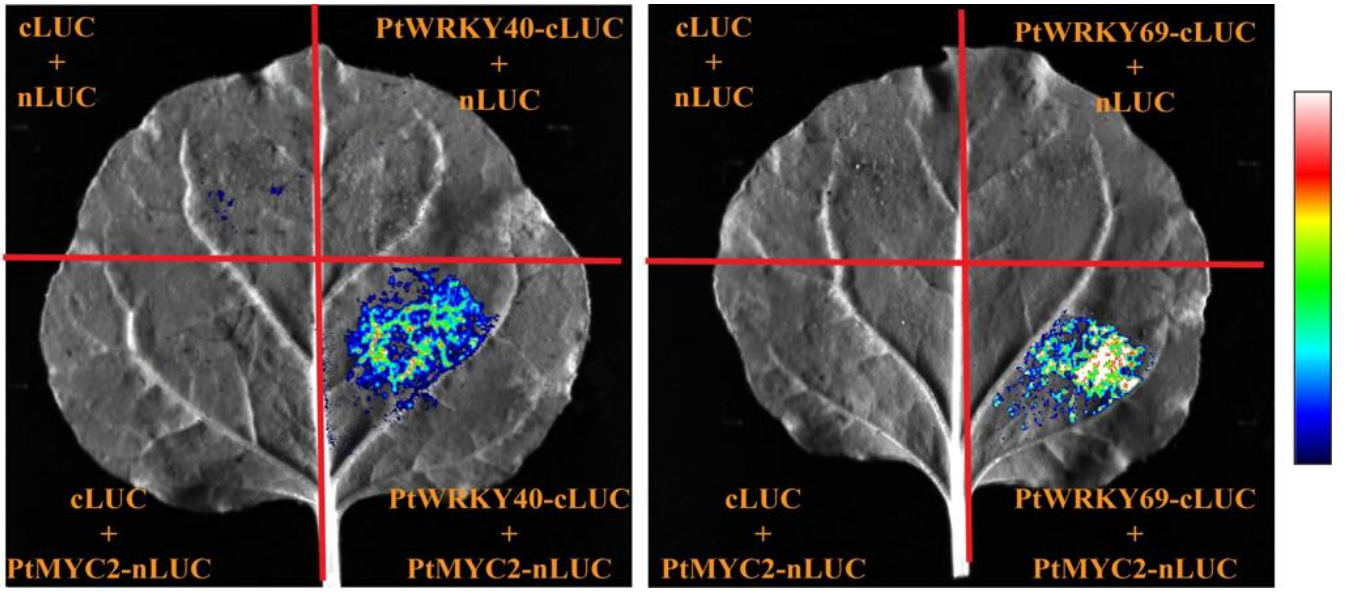


Fig. 6: Luciferase complementation imaging (LCI) assays of the interactions between PtWRKY40/PtWRKY69 and PtMYC2 in *N.benthamiana* leaves.Agrobacterium suspensions harboring the corresponding recombinant constructs were mixed in equal volumes and co-infiltrated into *N. benthamiana* leaves. At 48 h post-infiltration (hpi), the luminescence signals were captured and recorded.

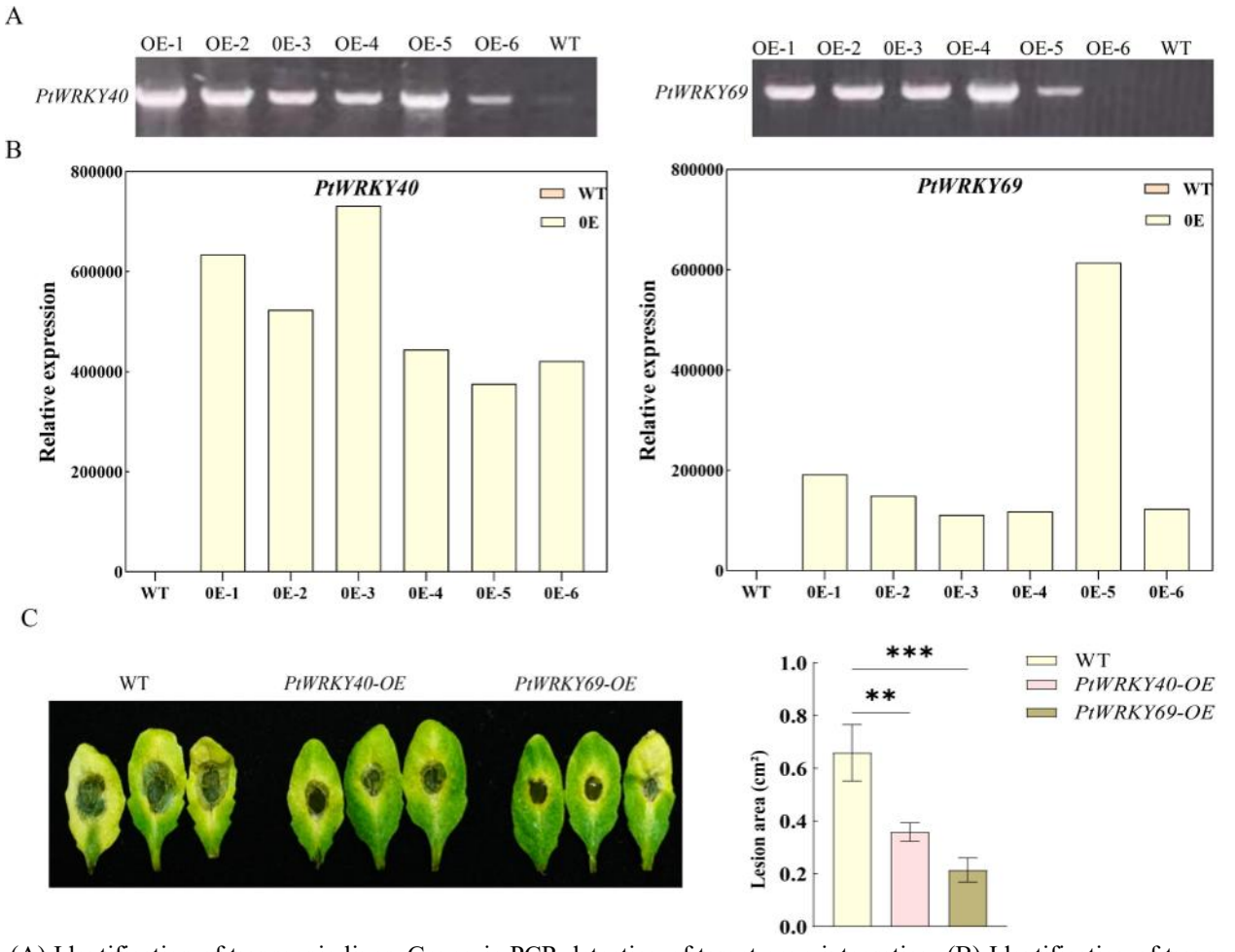


Fig. 7: (A) Identification of transgenic lines. Genomic PCR detection of target gene integration. (B) Identification of transgenic lines. Expression levels of the target genes detected by qRT-PCR. (C) Phenotypes of *Arabidopsis* wild-type (WT) and overexpression lines (*W40-OE* and *W69-OE*) at 5-7 days post-inoculation (dpi) with *F.oxysporum*. Data are expressed as mean ± SD. Asterisks indicate significant differences compared with WT (**P < 0.01, ***P < 0.001).

treatment groups (*W40-OE* and *W69-OE*) and the control group (WT). The sequencing generated a total of 55.2 Gb of clean reads, with each sample yielding over 5.5 Gb of clean reads. All 24,292 unigenes were annotated against the NR, Swiss-Prot, Pfam, eggNOG, GO, and KEGG databases. Specifically, 23,742 genes were annotated based on the NR database, 19,653 in Swiss-Prot, 19,701 in Pfam, 22,656 in eggNOG, and 22,437 in the GO database; additionally, 11,594 genes were functionally annotated based on the KEGG database. Principal component analysis (PCA) of the gene expression profiles from the nine samples (Fig. 8E) demonstrated high reproducibility within each group. The treatment groups and the control group were clearly separated along the PC1 axis, indicating significant differences in gene expression between the overexpression transgenic plants and the CK plants, with the primary variance (45.9%) explained by PC1.Correlation heatmap and hierarchical clustering analysis revealed high correlation among replicates within each group, indicating good experimental reproducibility (Fig. 8F).

To better understand the biological functions of the DEGs, GO and KEGG enrichment analyses were performed to functionally categorize the DEGs from the two comparison groups. All these DEGs were classified into three main functional categories: biological process (BP), cellular component (CC), and molecular function (MF). The GO enrichment analysis revealed that in the biological process (BP) category, the DEGs were significantly enriched in "cellular process", "metabolic process", and "response to stimulus". Within the cellular component (CC) category, "cell part", "organelle", and "membrane" were the primary enriched terms for the DEGs. Regarding molecular function (MF), the DEGs were predominantly enriched in "binding" and "catalytic activity". In the KEGG annotation database, the categories with the most assigned terms were "Metabolism" and "Genetic Information Processing". In the *W40-OE* vs. WT comparison group (Fig. 8B), "Oxidative phosphorylation", "Glucosinolate biosynthesis", "Plant-pathogen interaction", and "Phenylpropanoid biosynthesis" were significantly enriched in KEGG pathways. Meanwhile, GO database annotation indicated that terms including "response to oxygen-containing compound", "response to chemical", and "oxoacid metabolic process" were significantly enriched (Fig. 8A). In the *W69-OE* vs. WT comparison group, pathways such as

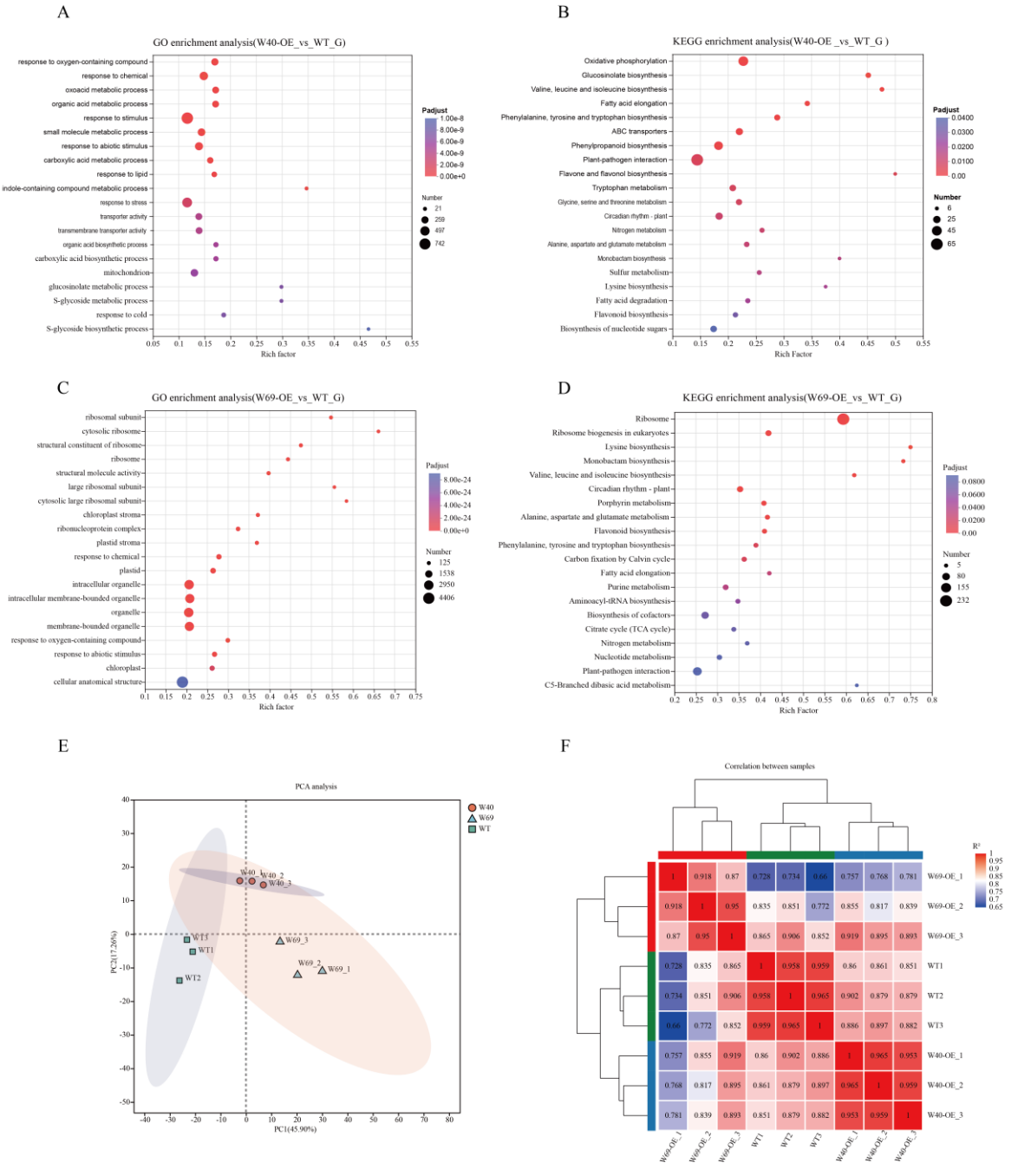


Fig. 8: Functional enrichment and expression profiling of W40-OE and W69-OE samples.(A–B) Gene Ontology (GO) and KEGG pathway enrichment analyses of unigenes in W40-OE.(C–D) Gene Ontology (GO) and KEGG pathway enrichment analyses of unigenes in W69-OE. (E) PCA of the samples. (F) Heatmap of sample correlations.

"Ribosome", "Lysine biosynthesis", "Circadian rhythm - plant", and "Flavonoid biosynthesis" were enriched in the KEGG database (Fig. 8D); in the GO database (Fig. 8C), the DEGs were enriched in terms including "ribosomal subunit", "chloroplast stroma", and "response to abiotic stimulus".

3.6.2 Expression patterns of disease resistance-related functional genes in *W40-OE* and *W69-OE*

To characterize the complex biological processes of the transcriptome and explore the potential disease resistance mechanisms of WRKY transcription factors, we performed KEGG pathway enrichment analysis on all DEGs from the two differentially expressed gene sets. The enrichment results revealed that in the *W40-OE* vs. WT comparison group, disease resistance-related pathways such as "Plant-pathogen interaction", "Phenylpropanoid biosynthesis", and "Flavone and flavonol biosynthesis" were significantly enriched (Fig. 8B), indicating that *PtWRKY40* may be directly involved in the resistance against pathogens. In the *W69-OE* vs. WT comparison group(Fig. 8D), DEGs were primarily enriched in pathways including "Plant-pathogen interaction", "Phenylalanine, tyrosine and tryptophan biosynthesis",

"Flavonoid biosynthesis", and "Porphyrin metabolism". These biological processes exert major regulatory roles in the *Arabidopsis* overexpressing *PtWRKY40* and *PtWRKY69*, participating in the disease resistance response either directly or indirectly through downstream defense networks.

We focused our analysis on the differential gene expression within the "Plant-pathogen interaction" pathway. In both the *W40* and *W69* genotypes (Fig. 9A, F), pattern recognition receptors (*FLS2*, *CERK1*, and *BAK1*); genes related to calcium signaling and MAPK cascades (*CML*, *CPK*, and *MPK4*); and *HSP90* family members responsible for stabilizing immune signaling complexes (*HSP90A*, *HSP90B*, and *htpG*) were all upregulated. Furthermore, NLR-type receptors (*RPS4* and *RPS5*), along with WRKY transcription factors that are broadly involved in defense responses, also exhibited an upregulation trend. Genes related to metabolism and oxidative regulation, including *KCS*, *NOA1*, *ECI3*, *HCD1*, tuf, and *TUFM-1*, were similarly upregulated.

The differentially expressed genes (DEGs) in both *W40-OE* and *W69-OE Arabidopsis* were enriched in the "Flavonoid biosynthesis" pathway, but the specifically upregulated genes differed between the two genotypes. In the *W40-OE* genotype, key genes for flavonoid synthesis, including *CYP75B1* and *UGT78D1* (Fig. 9B), as well as core genes for phenylpropanoid biosynthesis, such as *PAL*, and *HCT* , were all upregulated. Additionally, genes related to lignin biosynthesis, including *CCR*, *CAD*, *CSE*, *COMT*, also exhibited upregulation; the key enzymes for phenylpropanoid

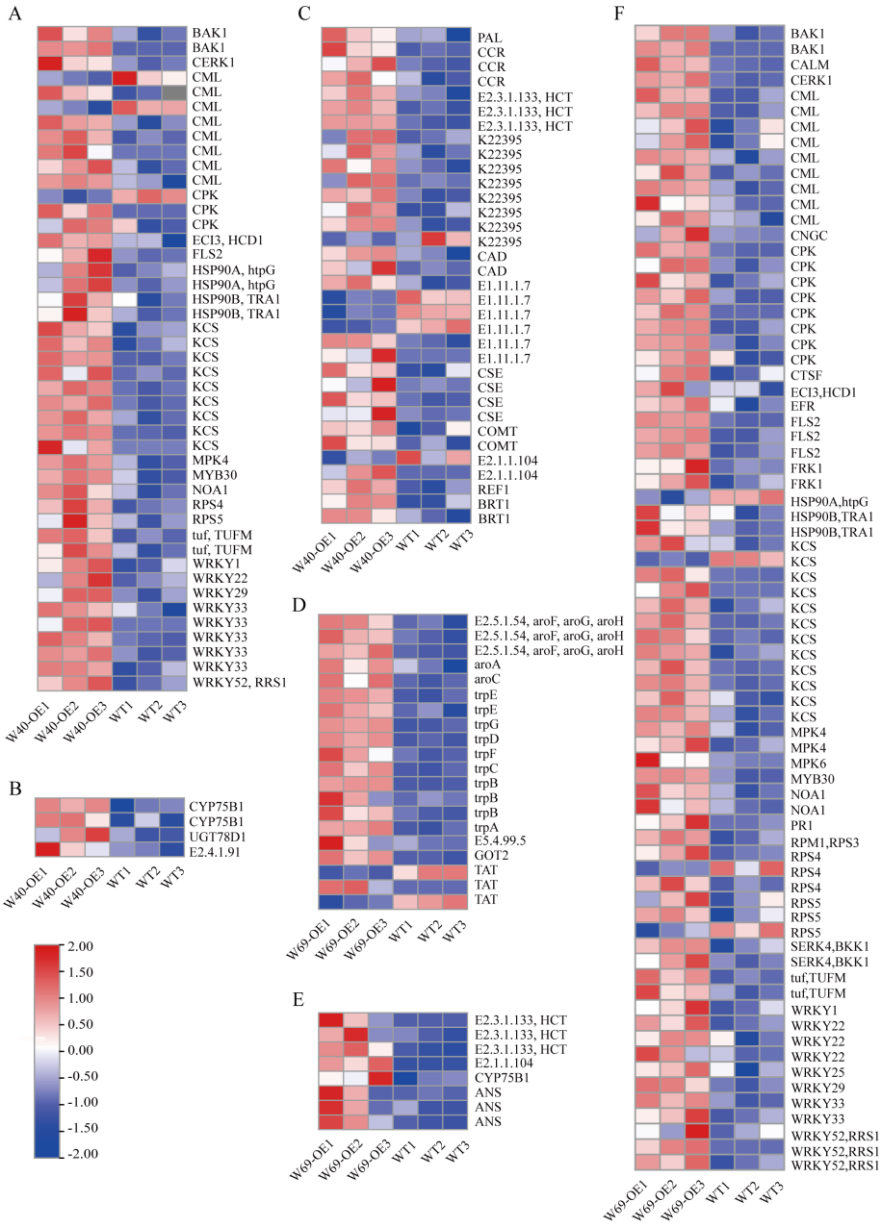


Fig. 9: Heatmaps of differentially expressed genes in *PtWRKY40-OE* and *PtWRKY69-OE Arabidopsis*. (A-C) Genes involved in the plant-pathogen interaction, flavonoid biosynthesis, and phenylpropanoid biosynthesis pathways in the *PtWRKY40-OE* genotype. (D-F) Genes involved in the phenylalanine, tyrosine and tryptophan biosynthesis, flavonoid biosynthesis, and plant-pathogen interaction pathways in the *PtWRKY69-OE* genotype.

derivative metabolism, *REF1* and *BRT1*, showed an upregulation trend (Fig. 9C).

Compared to the *W40-OE* genotype, the upregulated genes within the Flavonoid biosynthesis pathway in the *W69-OE* genotype included *HCT*, *CYP75B1*, and *ANS* (Fig. 9E), which collectively constitute a hierarchical regulatory system for flavonoid metabolism. KEGG enrichment analysis of the differentially expressed genes in the *W69-OE* vs. WT comparison group revealed a significant enrichment in the Phenylalanine, tyrosine and tryptophan biosynthesis pathway. Within this pathway, a total of 14 key genes, namely *aroF*, *aroG*, *aroH*, *aroA*, *aroC*, *trpE*, *trpG*, *trpD*, *trpF*, *trpC*, *trpB*, *trpA*, *GOT2*, and *TAT*, were significantly upregulated (Fig. 9D). Their functions cover various stages of the biosynthesis of aromatic amino acids (phenylalanine, tyrosine, and tryptophan).

4. Discussion

4.1 Pivotal role of WRKY transcription factors in plant disease immunity mediated by JA/SA hormone signaling

As one of the largest transcription factor families in plants, the WRKY transcription factor family regulates target gene expression by specifically recognizing the W-box cis-acting element (core sequence TTGACT/C), playing a key nodal role in plant hormone-mediated disease resistance responses.[12,23,24] In the jasmonic acid (JA) signaling pathway, WRKY transcription factors can affect hormone accumulation levels by regulating JA biosynthesis[25] and can also act as transcriptional regulators downstream of JA signaling to activate the expression of defense genes,[24] thereby linking pathogen recognition with immune responses. In the plant immune system, the jasmonic acid (JA) and salicylic acid (SA) signaling pathways form a division of defense mechanisms against pathogens with different trophic lifestyles: JA/ethylene-mediated defense is primarily directed against necrotrophic pathogens (necrotrophs), such as *Botrytis cinerea*,[26] inducing induced systemic resistance (ISR); whereas the SA-mediated defense response is mainly directed against biotrophic pathogens (biotrophs), such as *Pseudomonas syringae*,[27] regulating systemic acquired resistance (SAR).[8,9]

F.oxysporum, the primary causal pathogen of root rot in *P.tunicoides*, is a hemibiotrophic fungus.[28] During the initial stage of infection, it exhibits a biotrophic phase, and later transitions into a necrotrophic phase, obtaining nutrients by killing host cells and causing severe damage to the roots.[29] In this study, two WRKY transcription factors, *PtWRKY40* and *PtWRKY69*, which respond to pathogen infection, were screened from transcriptome data to elucidate their functions in the disease resistance response mediated by the JA signaling pathway. WRKY transcription factors play multiple roles in plant immune responses, and their family members often exhibit spatiotemporal expression specificity. In our study, *PtWRKY40* was strongly induced at the early stage of infection (3h) and reached its peak at 6h, whereas *PtWRKY69* showed specific upregulation at 6h. This differential induction pattern suggests that the two may function at distinct stages of the disease resistance response. Similar time-specific expression has also been reported in model plants. For instance, *Arabidopsis AtWRKY33* is rapidly activated following infection by *Botrytis cinerea* (a necrotroph),[30] while the induction of *AtWRKY75* is relatively delayed;[31] however, both participate in the defense against necrotrophic pathogens by regulating JA signaling.

Hormone measurement results indicated that *F.oxysporum* infection led to a significant increase in JA content ($P < 0.01$) in the roots of *P.tunicoides*, while the contents of SA and its metabolites (MESA and SAG) were significantly decreased ($P < 0.05$). This JA upward/SA downward (JA↑/SA↓) hormonal change is consistent with the plant defense response pattern against the late necrotrophic stage of hemibiotrophic pathogens. *F.oxysporum* transitions into a necrotrophic phase during the late stage of infection,[32] at which point the JA-mediated defense response exerts a more effective inhibitory effect against it. When a plant recognizes that a pathogen has entered the necrotrophic stage, it typically prioritizes the activation of the JA pathway and suppresses the SA pathway to optimize the allocation of defense resources.[33] The WRKY transcription factor family plays a pivotal role in this process; for instance, *Arabidopsis AtWRKY70* has been demonstrated to act as a convergence node for the SA and JA signaling pathways, with its expression being differentially regulated by the two hormones.[34] Although this study did not directly verify the regulatory effects of *PtWRKY40/69* on the SA pathway, the significant increase in JA content coupled with the synchronous decrease in SA content implies that these two WRKY members may participate in the crosstalk regulation of JA-SA signaling.

At the level of JA signal transduction, experimental results showed that *COI1* (the JA receptor) and *MYC2* (a bHLH transcription factor) were significantly upregulated at the early stage post-inoculation. The upregulation of *COI1* indicates that the JA signal perception mechanism was rapidly activated following pathogen recognition, while the induction of *MYC2* marks the transduction of JA signaling to downstream defense genes. As a core regulatory factor of the JA signaling pathway, *MYC*2 can activate the expression of various downstream defense-related genes.[35] Notably, the expression peak of *PtWRKY40* coincided closely with the activation timing of the JA biosynthesis gene *AOC/AOC3* and the signal transduction factor *MYC2*. This expression correlation suggests that *PtWRKY40* may participate in the JA-mediated early defense response and also implies that *P.tunicoides* may achieve fine-tuned regulation of the JA pathway through combinations of different WRKY members.

Furthermore, the additional subcellular localization results in this study revealed that the fluorescence signals of both *PtWRKY40* and *PtWRKY69* were predominantly distributed in the nucleus. This is consistent with their functional attributes as transcriptional regulatory proteins, providing a cytological

basis for their involvement in the expression regulation of pathogen-responsive genes. Further yeast two-hybrid (Y2H), bimolecular fluorescence complementation (BiFC), and luciferase complementation imaging (LCI) assays demonstrated that both *PtWRKY40* and *PtWRKY69* could interact with PtMYC2, a core transcription factor in the jasmonic acid (JA) signaling pathway, and the reconstituted BiFC fluorescence signals were primarily localized in the nucleus. These results indicate that *PtWRKY40*/*PtWRKY69* and PtMYC2 not only exhibit consistency in their temporal expression patterns but also interact directly at the protein level, thereby further strengthening the evidence for their potential co-involvement in the JA-related defense regulatory network.

In this study, the heterologous expression system in *Arabidopsis* was employed to verify the disease resistance functions of *PtWRKY40* and *PtWRKY69*. The results demonstrated that overexpression of these two genes significantly reduced the disease index after inoculation ($P < 0.01$). Since the genetic transformation system for *P.tunicoides* has not yet been established, Currently, less than 0.1% of higher plant species are amenable to efficient genetic transformation, and the situation is even more challenging for medicinal plants.[36] utilizing model plants such as *Arabidopsis* or tobacco for heterologous expression has become an effective alternative for verifying gene functions in medicinal plants. For example, the disease resistance functions of WRKY genes from medicinal plants, such as *AhWRKY33* from *Asarum heterotropoides*[37] and *McWRKY57* from Mentha canadensis,[38] have been validated through heterologous expression in *Arabidopsis*. In our experiments, we inoculated *Arabidopsis* plants with the pathogen and quantified the lesion sizes to validate the disease resistance functions of the two WRKY transcription factors. Under the current experimental conditions, heterologous expression in *Arabidopsis* represents the most feasible strategy to verify their roles in disease resistance.The results of this study expand our understanding of the functions of WRKY transcription factors in medicinal plants.

Compared with model plants, medicinal plants often possess unique secondary metabolic characteristics and specialized defense mechanisms. As a monotypic genus in the Caryophyllaceae family, the WRKY-JA regulatory module of *Psammosilene tunicoides* may have undergone adaptive evolution to cope with infection by root rot pathogens. This study provides a theoretical basis for utilizing model plants to study disease resistance mechanisms in medicinal plants. However, WRKY genes in medicinal plants may also possess species-specific functions. For instance, this study found that the specific induction pattern of *PtWRKY69* at 6 h is similar to that of *Arabidopsis AtWRKY57*,[38] yet functionally it acts as a positive regulator rather than a negative one. This discrepancy may stem from variations in gene sequences or differences in regulatory networks.

In conclusion, this study identified two key WRKY transcription factors, *PtWRKY40* and *PtWRKY69*, that respond to root rot pathogen infection in *P.tunicoides*. Our results revealed that following inoculation with *F.oxysporum*, both the levels of jasmonate (JA) phytohormones and the expression of JA pathway-related genes were significantly elevated in Psammosilene tunicoides, accompanied by the strong induction of the transcription factors *PtWRKY40* and *PtWRKY69*. Additionally, protein-protein interaction assays demonstrated that these two WRKY transcription factors interact with Pt*MYC2*. Phenotypic analyses based on heterologous expression in Arabidopsis confirmed that the overexpression of *PtWRKY40* and *PtWRKY69* enhanced plant resistance to *F. oxysporum*. Therefore, we hypothesize that these two WRKY transcription factors may be involved in the JA signaling pathway to mediate defense responses against root rot in *P. tunicoides*. These findings not only deepen our understanding of the functions of WRKY transcription factors in medicinal plants but also provide crucial candidate gene resources for the molecular breeding of disease resistance in *P. tunicoides*. The findings not only enrich the functional understanding of WRKY transcription factors in medicinal plants but also provide important candidate gene resources for the molecular breeding of disease resistance in *P. tunicoides*.

Although the current study provides multidimensional evidence - including hormonal changes, expression responses, subcellular localization, protein interactions, and heterologous expression in Arabidopsis - supporting the involvement of *PtWRKY40* and *PtWRKY69* in the resistance of *P.tunicoides* to root rot, certain limitations remain. First, functional validation was primarily conducted using an *Arabidopsis* heterologous expression system, as stable genetic transformation or reverse genetic approaches in *P. tunicoides* have not yet been established. Therefore, *PtWRKY40* and *PtWRKY69* are currently best considered as highly supported candidate regulatory factors for disease resistance. Second, although yeast two-hybrid (Y2H), BiFC, and LCI assays have demonstrated definite protein interactions between *PtWRKY40*/*PtWRKY69* and PtMYC2, further experiments, such as ChIP-qPCR, are required to determine whether they directly regulate downstream target genes within the jasmonic acid (JA) pathway. Furthermore, the transcriptional activation activities of *PtWRKY40* and *PtWRKY69* have not yet been experimentally determined, leaving their precise modes of action as transcriptional regulators to be fully elucidated. To address this limitation, our future studies will prioritize the use of yeast one-hybrid (Y1H) assays to verify their binding specificity to potential target gene promoters, coupled with in vivo dual-luciferase (Dual-LUC) reporter assays to systematically evaluate their transcriptional activation or repression activities. Ultimately, integrating the establishment of a genetic transformation system in *P. tunicoides* with direct target gene verification and transcriptional activity analyses will comprehensively elucidate the molecular mechanisms of the *PtWRKY40*/*PtWRKY69*–PtMYC2 regulatory module.

4.2 Differences in disease resistance strategies between *W40* and *W69* genotype *Arabidopsis*

The plant-pathogen interaction pathway is the core signaling network for plant defense against pathogen invasion, and its precise regulation directly determines the disease resistance of the plant.[39] This pathway primarily relies on two layers of synergistically operating immune systems: the first line of defense is pattern-triggered immunity (PTI) triggered by the recognition of pathogen-associated molecular patterns (PAMPs) by cell surface pattern recognition receptors (PRRs); the second line of defense is effector-triggered immunity (ETI) triggered by the specific recognition of pathogen effector proteins by intracellular nucleotide-binding leucine-rich repeat receptors (NLRs).[40] The initiation of PTI and ETI is accompanied by a series of complex signaling cascades, including transient changes in intracellular calcium flux, bursts of reactive oxygen species (ROS), activation of the MAPK cascade pathway, and the synthesis of defense hormones (such as salicylic acid and jasmonic acid), which synergistically regulate the expression of downstream defense genes. Compared to the wild type (WT), the differentially expressed genes (DEGs) in both the *W40-OE* and *W69-OE* transgenic lines were significantly enriched in the plant-pathogen interaction pathway, indicating that this signaling network plays a leading role in responding to pathogen stress. Expression profiling analysis revealed that genes encoding receptors and co-receptors responsible for PAMP perception (*FLS2*, *CERK1*, and *BAK*1) were significantly upregulated in the overexpression lines, providing a foundation for the host to initiate early PTI defense.[41] Furthermore, the high expression of NLR-type resistance genes such as *RPS4* and *RPS5* further amplified the intensity of the ETI response, which facilitates the accelerated formation of the hypersensitive response (HR), thereby effectively blocking the colonization and spread of pathogens.

The phenylpropanoid biosynthesis and flavonoid biosynthesis pathways constitute core branches of plant secondary metabolism and play pivotal roles in resistance to pathogen infection.[42,43] Upon pathogen invasion, the *W40-OE* genotype rapidly activates immune signaling, thereby systemically inducing these metabolic networks and enhancing the efficiency and capacity of the plant defense response. At the level of chemical defense, the upregulation of flavonoid biosynthesis-related genes, including *CYP75B1* and *UGT78D1*, promotes the hydroxylation and glycosylation of the flavonoid backbone, leading to the accumulation of flavonoids and their derivatives.[44,45] At the level of physical defense, the increased expression of key genes in the phenylpropanoid pathway, such as *PAL*, *CCR*, and *CAD*, facilitates lignin deposition in the cell wall, thereby strengthening the physical barrier and effectively restricting pathogen invasion and spread.[46] Meanwhile, this pathway also provides precursors for the biosynthesis of antimicrobial compounds, including flavonoids, phenolics, and phytoalexins. These metabolites not only directly inhibit pathogen growth, but also participate in the regulation of other defense-related pathways in plants. This result is highly consistent with the significant enrichment of the Plant–pathogen interaction, Phenylpropanoid biosynthesis, and Flavone biosynthesis pathways in the *W40-OE* genotype, suggesting that the *W40* genotype is able to rapidly activate immune signaling and coordinately induce the flavonoid and phenylpropanoid metabolic networks, thereby enhancing both the speed and effectiveness of the plant defense response against pathogen invasion.

In the *W69-OE* genotype, the upregulation of multiple key genes in the "Phenylalanine, tyrosine and tryptophan biosynthesis" and "Flavonoid biosynthesis" pathways is of great significance. In the aromatic amino acid biosynthesis pathway, the upregulated genes (such as *aroF*, *aroG*, *aroH*, *aroA*, *aroC*, *trpE*, *trpG*, *trpD*, *trpF*, *trpC*, *trpB*, *trpA*, *GOT2*, and *TAT*) promote the accumulation of phenylalanine, tyrosine, and tryptophan, providing sufficient precursor materials for the synthesis of flavonoids.[47] In the flavonoid biosynthesis pathway, upregulated genes such as *CYP75B1* and *ANS* act as key enzymes, whereas *HCT* is primarily involved in lignin precursor formation.[48,49] The synergistic upregulation of these genes not only increases the accumulation of plant chemical defense substances but also strengthens the physical barrier of the cell wall through lignin deposition, enabling the plant to exert both chemical and physical defense roles under pathogen infection, thereby improving overall disease resistance.

Through the enrichment analysis of differentially expressed genes and functional studies of key genes, this study compared the molecular mechanisms of disease resistance between *PtWRKY40 (W40-OE)* and *PtWRKY69 (W69-OE)*. The results showed that the synergistic activation of both in the "Plant-pathogen interaction" and "Flavonoid biosynthesis" pathways forms a multi-level disease resistance system characterized by the synergy of signal perception and chemical defense: the former is responsible for pathogen recognition and immune signal transduction, while the latter achieves antibacterial, antioxidant, and cell wall reinforcement through the synthesis of flavonoids. Furthermore, the *W40-OE* genotype enhances plant resistance to pathogens by activating the phenylpropanoid metabolic pathway to promote the accumulation of flavonoids, thereby providing synergistic reinforcement through both physical barriers and chemical defense. In contrast, the *W69-OE* genotype relies on the regulation of the aromatic amino acid pathway to provide sufficient precursors for flavonoids and other disease-resistance substances. In summary, WRKY family genes exhibit diversity in regulating plant disease resistance responses, providing a theoretical basis for elucidating the disease resistance mechanisms of different genotypes and screening candidate genes for disease resistance breeding.

5. Conclusion

In conclusion, this study identified two key WRKY transcription factors, *PtWRKY40* and *PtWRKY69*, that respond

to root rot pathogen infection in *P. tunicoides*. Our results revealed that following inoculation with *F. oxysporum*, both the levels of jasmonate (JA) phytohormones and the expression of JA pathway-related genes were significantly elevated in Psammosilene tunicoides, accompanied by the strong induction of the transcription factors *PtWRKY40* and *PtWRKY69*. Additionally, protein-protein interaction assays demonstrated that these two WRKY transcription factors interact with *PtMYC2*. Phenotypic analyses based on heterologous expression in Arabidopsis confirmed that the overexpression of *PtWRKY40* and *PtWRKY69* enhanced plant resistance to *F. oxysporum*. Therefore, we hypothesize that these two WRKY transcription factors may be involved in the JA signaling pathway to mediate defense responses against root rot in *P. tunicoides*. These findings not only deepen our understanding of the functions of WRKY transcription factors in medicinal plants but also provide crucial candidate gene resources for the molecular breeding of disease resistance in *P. tunicoides*. The findings not only enrich the functional understanding of WRKY transcription factors in medicinal plants but also provide important candidate gene resources for the molecular breeding of disease resistance in *P. tunicoides*.

Acknowledgments

The authors declare that financial support was received for the research and publication of this article. This research was funded the National Natural Science Foundation of China (Grant No: 82460715), Program of Applied Basic Research in Yunnan Province (Grant Nos: 20254916CE340047, CMP2026OP-C18).

Conflict of Interest

There is no conflict of interest.

Supporting Information

Applicable.

CRediT Statement

Shuyun Qi: Investigation, Methodology, Formal analysis, Data curation, Visualization, Writing – Original draft. **Lijuan Wang:** Investigation, Methodology, Formal analysis, Data curation, Writing – Original draft. **Qiaofeng Li:** Investigation, Validation, Visualization. **Fei Ji:** Investigation, Validation, Resources. **Zhizhong Yang:** Conceptualization, Supervision, Project administration, Funding acquisition, Writing – Review & editing. **Guanghui Ni:** Methodology, Resources, Supervision, Writing – Review & editing. **Aili Zhang:** Conceptualization, Supervision, Project administration, Funding acquisition, Writing – Review & editing.

References

[1] W. T. Yang, G. D. Li, J. N. Li, C. F. Yang, X. M. Zhang, A. L. Zhang, Comparative analysis of rhizosphere and endophytic microbial communities between root rot and healthy root of psammosilene tunicoides, *Current Microbiology*, 2023, **80**, 215, doi: 10.1007/s00284-023-03290-4.

[2] J. Meng, L. Zhang, J. He, Y. Zhao, Complete plastid genome sequence of the rare and endangered medicinal herb *Psammosilene tunicoides*, endemic to China, *Mitochondrial DNA Part B*, 2019, **4**, 2343-2344, doi: 10.1080/23802359.2019.1629348.

[3] H. Qiu, L. Su, H. Wang, Z. Zhang, Chitosan elicitation of saponin accumulation in *Psammosilene tunicoides* hairy roots by modulating antioxidant activity, nitric oxide production and differential gene expression, *Plant Physiology and Biochemistry*, 2021, **166**, 115-127, doi: 10.1016/j.plaphy.2021.05.033.

[4] Y.-H. Li, X.-S. Bai, X.-X. Yang, Y.-X. Li, H.-R. Li, Z.-L. Wang, W. Wang, K. Tian, X.-Z. Huang, Triterpenoid saponins from *Psammosilene tunicoides* and their antinociceptive activities, *Phytochemistry*, 2023, **214**, 113795, doi: 10.1016/j.phytochem.2023.113795.

[5] A.-L. Zhang, Y.-F. Gao, G.-D. Li, Z.-G. Qian, Development, characterization, and cross-amplification of microsatellite markers for *Psammosilene Tunicoides* (Caryophyllaceae), *Applications in Plant Sciences*, 2018, **6**, e01199, doi: 10.1002/aps3.1199.

[6] Y. Li, Q. Li, L. Wang, S. Qi, Z. Jiang, W. Zhang, A. Zhang, Integrated analysis of transcriptomics and metabolomics and high-throughput amplicon sequencing reveals the synergistic effects of secondary metabolites and rhizosphere microbiota on root rot resistance in *Psammosilene tunicoides*, *Frontiers in Microbiology*, 2025, **16**, 1554406, doi: 10.3389/fmicb.2025.1554406.

[7] B. Sawicka, P. Barbaś, V. Vambol, D. Skiba, P. Pszczółkowski, P. Niazi, B. Bienia, Applied microbiology for sustainable agricultural development, *Applied Microbiology*, 2025, **5**, 78, doi: 10.3390/applmicrobiol5030078.

[8] T. Mengiste, C.-J. Liao, Contrasting mechanisms of defense against biotrophic and necrotrophic pathogens, 20 years later: what has changed?, *Annual Review of Phytopathology*, 2025, **63**, 279-308, doi: 10.1146/annurev-phyto-121823-031139.

[9] J. Glazebrook, Contrasting mechanisms of defense against biotrophic and necrotrophic pathogens, *Annual Review of Phytopathology*, 2005, **43**, 205-227, doi: 10.1146/annurev.phyto.43.040204.135923.

[10] I. Stenzel, M. Otto, C. Delker, N. Kirmse, D. Schmidt, O. Miersch, B. Hause, C. Wasternack, ALLENE OXIDE CYCLASE (AOC) gene family members of Arabidopsis thaliana: tissue- and organ-specific promoter activities and *in vivo* heteromerization, *Journal of Experimental Botany*, 2012, **63**, 6125-6138, doi: 10.1093/jxb/ers261.

[11] J. Ruan, Y. Zhou, M. Zhou, J. Yan, M. Khurshid, W. Weng, J. Cheng, K. Zhang, Jasmonic acid signaling pathway in plants, *International Journal of Molecular Sciences*, 2019, **20**, 2479, doi: 10.3390/ijms20102479.

[12] J. Jiang, S. Ma, N. Ye, M. Jiang, J. Cao, J. Zhang, WRKY transcription factors in plant responses to stresses, *Journal of Integrative Plant Biology*, 2017, **59**, 86-101, doi: 10.1111/jipb.12513.

[13] S. H. Wani, S. Anand, B. Singh, A. Bohra, R. Joshi, WRKY

transcription factors and plant defense responses: latest discoveries and future prospects, *Plant Cell Reports*, 2021, **40**, 1071-1085, doi: 10.1007/s00299-021-02691-8.
[14] L. Su, L. Zheng, H. Wang, Y. Qu, F. Ge, D. Liu, Panax notoginseng transcription factor WRKY15 modulates resistance to Fusarium solani by up-regulating osmotin-like protein expression and inducing JA/SA signaling pathways, *BioMed Central Plant Biology*, 2023, **23**, 362, doi: 10.1186/s12870-023-04373-x.
[15] H. Huang, W. Zhao, H. Qiao, C. Li, L. Sun, R. Yang, X. Ma, J. Ma, S. Song, S. Wang, SlWRKY45 interacts with jasmonate-ZIM domain proteins to negatively regulate defense against the root-knot nematode *Meloidogyne incognita* in tomato, *Horticulture Research*, 2022, **9**, uhac197, doi: 10.1093/hr/uhac197.
[16] M. Skibbe, N. Qu, I. Galis, I. T. Baldwin, Induced plant defenses in the natural environment: *Nicotiana attenuata*WRKY3 and WRKY6 coordinate responses to herbivory, *The Plant Cell*, 2008, **20**, 1984-2000, doi: 10.1105/tpc.108.058594.
[17] P. J. Rushton, I. E. Somssich, P. Ringler, Q. J. Shen, WRKY transcription factors, *Trends in Plant Science*, 2010, **15**, 247-258, doi: 10.1016/j.tplants.2010.02.006.
[18] R. P. Birkenbihl, C. Diezel, I. E. Somssich, Arabidopsis WRKY33 is a key transcriptional regulator of hormonal and metabolic responses toward*Botrytis cinerea*Infection, *Plant Physiology*, 2012, **159**, 266-285, doi: 10.1104/pp.111.192641.
[19] X. Wang, J. Li, J. Guo, Q. Qiao, X. Guo, Y. Ma, The WRKY transcription factor PlWRKY65 enhances the resistance of Paeonia lactiflora (herbaceous peony) to Alternaria tenuissima, *Horticulture Research*, 2020, **7**, 57, doi: 10.1038/s41438-020-0267-7.
[20] W. T. Yang, X. M. Zhang, G. D. Li, J. N. Li, C. F. Yang, A. L. Zhang, Isolation and identification of pathogens causing root rot disease of Psammosilene tunicoides in Yunnan Province, *Guihaia*, 2023, **43**, 79-87, doi: 10.11931/guihaia.gxzw202205027.
[21] K. J. Livak, T. D. Schmittgen, Analysis of relative gene expression data using real-time quantitative PCR and the 2–ΔΔCT method, *Methods*, 2001, **25**, 402-408, doi: 10.1006/meth.2001.1262.
[22] K. Zhao, X. Wu, G. Han, L. Sun, C. Zheng, H. Hou, B. B. Xu, Z. M. El-Bahy, C. Qian, M. Kallel, H. Algadi, Z. Guo, Z. Shi, Phyllostachys nigra (Lodd. ex Lindl.) derived polysaccharide with enhanced glycolipid metabolism regulation and mice gut microbiome, *International Journal of Biological Macromolecules*, 2024, **257**, 128588, doi: 10.1016/j.ijbiomac.2023.128588.
[23] T. Eulgem, P. J. Rushton, S. Robatzek, I. E. Somssich, The WRKY superfamily of plant transcription factors, *Trends in Plant Science*, 2000, **5**, 199-206, doi: 10.1016/s1360-1385(00)01600-9.
[24] B. Saha, J. Nayak, R. Srivastava, S. Samal, D. Kumar, J. Chanwala, N. Dey, M. K. Giri, Unraveling the involvement of WRKY TFs in regulating plant disease defense signaling, *Planta*, 2023, **259**, 7, doi: 10.1007/s00425-023-04269-y.
[25] X. Peng, Y. Hu, X. Tang, P. Zhou, X. Deng, H. Wang, Z. Guo, Constitutive expression of rice WRKY30 gene increases the endogenous jasmonic acid accumulation, PR gene expression and resistance to fungal pathogens in rice, *Planta*, 2012, **236**, 1485-1498, doi: 10.1007/s00425-012-1698-7.
[26] A. Samaras, G. S. Karaoglanidis, G. Tzelepis, Insights into the multitrophic interactions between the biocontrol agent Bacillus subtilis MBI 600, the pathogen *Botrytis cinerea* and their plant host, *Microbiological Research*, 2021, **248**, 126752, doi: 10.1016/j.micres.2021.126752.
[27] J. Blomberg, V. Tasselius, A. Vergara, F. Karamat, Q. M. Imran, Å. Strand, M. Rosvall, S. Björklund, Pseudomonas syringae infectivity correlates to altered transcript and metabolite levels of Arabidopsis mediator mutants, *Scientific Reports*, 2024, **14**, 6771, doi: 10.1038/s41598-024-57192-x.
[28] Y. C. Chen, B. N. Kidd, L. C. Carvalhais, P. M. Schenk, Molecular defense responses in roots and the rhizosphere against *Fusarium oxysporum*, *Plant Signaling & Behavior*, 2014, **9**, e977710, doi: 10.4161/15592324.2014.977710.
[29] C. B. Michielse, M. Rep, Pathogen profile update: *Fusarium oxysporum*, *Molecular Plant Pathology*, 2009, **10**, 311-324, doi: 10.1111/j.1364-3703.2009.00538.x.
[30] Z. Zheng, S. Abu Qamar, Z. Chen, T. Mengiste, Arabidopsis WRKY33 transcription factor is required for resistance to necrotrophic fungal pathogens, *The Plant Journal*, 2006, **48**, 592-605, doi: 10.1111/j.1365-313x.2006.02901.x.
[31] L. Chen, L. Zhang, S. Xiang, Y. Chen, H. Zhang, D. Yu, The transcription factor WRKY75 positively regulates jasmonate-mediated plant defense to necrotrophic fungal pathogens, *Journal of Experimental Botany*, 2021, **72**, 1473-1489, doi: 10.1093/jxb/eraa529.
[32] R. Lyons, J. Stiller, J. Powell, A. Rusu, J. M. Manners, K. Kazan, *Fusarium oxysporum* triggers tissue-specific transcriptional reprogramming in Arabidopsis thaliana, *Public Library of Science One*, 2015, **10**, e0121902, doi: 10.1371/journal.pone.0121902.
[33] H. S. Kalsi, A. A. Karkhanis, B. Natarajan, A. J. Bhide, A. K. Banerjee, AUXIN RESPONSE FACTOR 16 (StARF16) regulates defense gene StNPR1 upon infection with necrotrophic pathogen in potato, *Plant Molecular Biology*, 2022, **109**, 13-28, doi: 10.1007/s11103-022-01261-0.
[34] J. Li, G. Brader, E. T. Palva, The WRKY70 transcription factor: a node of convergence for jasmonate-mediated and salicylate-mediated signals in plant defense, *The Plant Cell*, 2004, **16**, 319-331, doi: 10.1105/tpc.016980.
[35] B. Dombrecht, G. P. Xue, S. J. Sprague, J. A. Kirkegaard, J. J. Ross, J. B. Reid, G. P. Fitt, N. Sewelam, P. M. Schenk, J. M. Manners, K. Kazan, MYC_2 differentially modulates diverse jasmonate-dependent functions in *Arabidopsis*, *The Plant Cell*, 2007, **19**, 2225-2245, doi: 10.1105/tpc.106.048017.
[36] Y.-X. Niu, Q.-Y. Wu, S.-N. Ren, J. H. Won, H.-L. Wang, Developmental regulators and additives in promoting genetic transformation and genome editing efficiency, *Plant Physiology and Biochemistry*, 2026, **230**, 110811, doi: 10.1016/j.plaphy.2025.110811.

[37] Y.-C. Yang, X.-H. Wang, Y.-F. Wang, X.-Y. Liu, S.-H. Yang, Cloning of AhWRKY33 from *Asarum heterotropoides* and its genetic transformation in *Arabidopsis*, *China Journal of Chinese Materia Medica*, 2020, **45**, 3112-3119, doi: 10.19540/j.cnki.cjcmm.20200329.107.
[38] Y. Bai, T. Zhang, X. Zheng, B. Li, X. Qi, Y. Xu, L. Li, C. Liang, Overexpression of a WRKY transcription factor McWRKY57-like from Mentha canadensis L. enhances drought tolerance in transgenic Arabidopsis, *BioMed Central Plant Biology*, 2023, **23**, 216, doi: 10.1186/s12870-023-04213-y.
[39] Y. Jiang, D. Yu, The WRKY57 transcription factor affects the expression of jasmonate ZIM-domain genes transcriptionally to compromise *Botrytis cinerea* resistance, *Plant Physiology*, 2016, **171**, 2771-2782, doi: 10.1104/pp.16.00747.
[40] L.-N. Ding, Y.-T. Li, Y.-Z. Wu, T. Li, R. Geng, J. Cao, W. Zhang, X.-L. Tan, Plant disease resistance-related signaling pathways: recent progress and future prospects, *International Journal of Molecular Sciences*, 2022, **23**, 16200, doi: 10.3390/ijms232416200.
[41] J. Wang, J. Chai, Structural insights into the plant immune receptors PRRs and NLRs, *Plant Physiology*, 2020, **182**, 1566-1581, doi: 10.1104/pp.19.01252.
[42] D. Chinchilla, C. Zipfel, S. Robatzek, B. Kemmerling, T. Nürnberger, J. D. G. Jones, G. Felix, T. Boller, A flagellin-induced complex of the receptor FLS2 and BAK1 initiates plant defence, *Nature*, 2007, **448**, 497-500, doi: 10.1038/nature05999.
[43] R. L. Nicholson, R. Hammerschmidt, Phenolic compounds and their role in disease resistance, *Annual Review of Phytopathology*, 1992, **30**, 369-389, doi: 10.1146/annurev.py.30.090192.002101.
[44] R. A. Dixon, N. L. Paiva, Stress-induced phenylpropanoid metabolism, *The Plant Cell*, 1995, 1085-1097, doi: 10.1105/tpc.7.7.1085.
[45] M. J. Rao, Y. Xu, X. Tang, Y. Huang, J. Liu, X. Deng, Q. Xu, CsCYT75B1, a citrus CYTOCHROME P450 gene, is involved in accumulation of antioxidant flavonoids and induces drought tolerance in transgenic Arabidopsis, *Antioxidants*, 2020, **9**, 161, doi: 10.3390/antiox9020161.
[46] P. Jones, B. Messner, J.-I. Nakajima, A. R. Schäffner, K. Saito, UGT73C6 and UGT78D1, glycosyltransferases involved in flavonol glycoside biosynthesis in Arabidopsis thaliana, *Journal of Biological Chemistry*, 2003, **278**, 43910-43918, doi: 10.1074/jbc.m303523200.
[47] W. Boerjan, J. Ralph, M. Baucher, Lignin biosynthesis, *Annual Review of Plant Biology*, 2003, **54**, 519-546, doi: 10.1146/annurev.arplant.54.031902.134938.
[48] H. Maeda, N. Dudareva, The shikimate pathway and aromatic amino acid biosynthesis in plants, *Annual Review of Plant Biology*, 2012, **63**, 73-105, doi: 10.1146/annurev-arplant-042811-105439.
[49] Y. Mao, J. Luo, Z. Cai, Biosynthesis and regulatory mechanisms of plant flavonoids: a review, *Plants*, 2025, **14**, 1847, doi: 10.3390/plants14121847.

Publisher's Note: Engineered Science Publisher remains neutral with regard to jurisdictional claims in published maps and institutional affiliations.

Open Access
This article is licensed under a Creative Commons Attribution 4.0 International License, which permits the use, sharing, adaptation, distribution and reproduction in any medium or format, as long as appropriate credit to the original author(s) and the source is given by providing a link to the Creative Commons license and changes need to be indicated if there are any. The images or other third-party material in this article are included in the article's Creative Commons license, unless indicated otherwise in a credit line to the material. If material is not included in the article's Creative Commons license and your intended use is not permitted by statutory regulation or exceeds the permitted use, you will need to obtain permission directly from the copyright holder. To view a copy of this license, visit http://creativecommons.org/ licenses/by/4.0/.

©The Author(s) 2026.